University
of Glasgow

VIA VERITAS VITA

http://eprints.gla.ac.uk/69715/

Deposited on: 1 October 2012

TERRESTRIAL LASER SCAN ERROR IN THE PRESENCE OF DENSE GROUND VEGETATION

By SEAMUS COVENEY (seamus.coveney@nuim.ie),
National Centre for Geocomputation, NUI Maynooth, Ireland

and A. STEWART FOTHERINGHAM (stewart.fotheringham@nuim.ie)
National Centre for Geocomputation, NUI Maynooth, Ireland

Abstract

Terrestrial Laser Scan (TLS) data are seeing increasing use in geology, geomorphology, forestry and urban mapping. The ease of use, affordability and operational flexibility of TLS suggests that demand for it is likely to increase in large scale mapping studies. However, its advantages may remain restricted to specific environments, due to difficulties in defining bare-ground level in the presence of ground level vegetation. This paper seeks to clarify the component contributions to TLS elevation error deriving from vegetation occlusion, scan co-registration error, point-cloud georeferencing error and target position-definition in TLS point-cloud data. A very high-resolution (c.250 points/m^2) multi-scan single-returns TLS point-cloud data-set is acquired for an 11-hectare area of open, substantially flat and 100% vegetated coastal saltmarsh, providing data for the empirical quantification of TLS error. Errors deriving from the sources discussed are quantified, clarifying the potential proportional contribution of vegetation to other error sources. Initial data validation is applied to the TLS point-cloud data after application of a local-lowest-point selection process, and repeat validation tests are applied to the resulting filtered point-cloud after application of a kriging-based error-adjustment using a data fusion with GPS. The final results highlight the problem of representing bare-ground effectively within TLS data captured in the presence of dense ground vegetation and clarify the component contributions of elevation error deriving from surveying and data processing.

KEYWORDS: Terrestrial Laser Scanning, vegetation error, GPS data fusion.

INTRODUCTION

Terrestrial Laser Scanning

TLS is now capable of comparable performance to ALS in terms of operational range, ranging accuracy, pulse repetition frequency, laser pulse width, operational wavelengths and time segregation and waveform representation of laser returns (Petrie & Toth 2009). TLS also offers advantages in terms of ease of use, operational cost and freedom from the accuracy limitations associated with realtime georeferencing (Petrie & Toth 2009). The use of TLS in now well established in geology (Rosser et al. 2005, Buckley et al. 2008), forest inventory assessment (Schardt *et al.* 2002, Thies & Spiecker 2005, Henning & Radtke 2006, Danson et al. 2007) and urban mapping (Vosselman et al. 2004, Pu & Vosselman 2009). More recently, its potential in fluvial Geomorphology (Heritage & Herrington 2007), floodplain mapping (Straatsma et al. 2008) and wetland mapping (Guarnieri et al. 2009) have begun to be explored.

The problem of segregating canopy and ground laser returns in ALS data is widely known. The segregation of first and last laser returns (Lim et al., 2003, Hall et al., 2005; Webster, 2006) and analysis of full pulse waveform return (Nayegandhi et al., 2006, Wagner et al., 2008) can help to overcome the problem of identifying the bare ground surface in circumstances where full-footprint laser-pulse illumination of the ground surface is possible. The problem of occlusion of the bare ground surface by vegetation has been noted in a number of TLS studies (Heritage and Hetherington 2007, Pfeifer & Briese 2007). The scope for correcting elevation error associated with ground vegetation has also been explored. This research has included the use of external ground reference data and internal texture measures to correct error in vegetation canopies of varying depths (Pfeifer et al. 2004) the implementation of texture based correction in flat grassland / marshland areas (Gorte et al. 2005) and the use of GPS ground measurements to optimise window size for point cloud filtering in saltmarsh areas (Guarnieri et al. 2009).

This study applies a local-lowest point filter to the test data, prior to quantifying the magnitude of elevation error occurring in a densely vegetated saltmarsh using GPS elevation measurements. The filter is applied in this case primarily as a point-cloud reduction measure that simultaneously removes the highest local returns. GPS is used to quantify absolute elevation error in the filtered data, (and to subsequently correct) residual error. However, the primary aim is to highlight the proportional contribution of dense ground vegetation in comparison to elevation errors deriving from GPS error, scan co-registration error, geo-registration error and errors resulting from incorrect definition of the laser targets (termed henceforth, as 'laser target position-definition error').

Validation of Laser Scan data using GPS

ELEVATION errors within post-processed dual-frequency GPS and RTK dual frequency GPS measurements typically range from $\pm 0 \cdot 01$ to $< \pm 0 \cdot 1$ m (Gao & Chen, 2004; Fuller-Rowell, 2005). These errors are well within the (x3 and x5) accuracy differentials recommended by ASPRS (Flood, 2004) and EuroSDR (Höhle & Potuckova 2006) for accuracy validation of ALS data. GPS data have been used in a number of studies in order to validate ALS error (Baldi et al. 2002, Webster, 2005, Oksanen & Sarjakoski, 2006). The capability of GPS to acquire measurements at bare-ground level, and the high accuracies that can be achieved

with GPS make it particularly suitable for the validation of TLS data acquired in situations where ground vegetation cover masks the ground surface. Dual-frequency GPS survey data are used in this study (after the application of a local lowest point data filter) to externally validate elevation error in an 11-hectare TLS point-cloud data-set captured in an open saltmarsh grassland area.

Research Aims

THE PRINCIPAL AIM of this paper is to quantify the component contribution to total TLS elevation error arising from laser-pulse occlusion by ground vegetation, and to compare this with the contributions to overall TLS error deriving from GPS error, scan co-registration error, geo-registration error and laser target position-definition error. The impact of ground vegetation error is assessed using external post-processed and static Realtime Kinematic (RTK) GPS, and the magnitude of the errors deriving from all other sources is examined using separate GPS data and internal statistical measures.

METHODS

Selection of test area

THE TEST SITE (figure 1a) was selected from within an open, relatively-flat coastal saltmarsh grassland area that was characterised by 100% vegetation cover (figure 1b). The data were captured as part of an associated study (Coveney et al. 2010) in a flood-prone legislatively-protected habitat area where high-resolution TLS and GPS data were acquired in the absence of ALS data.
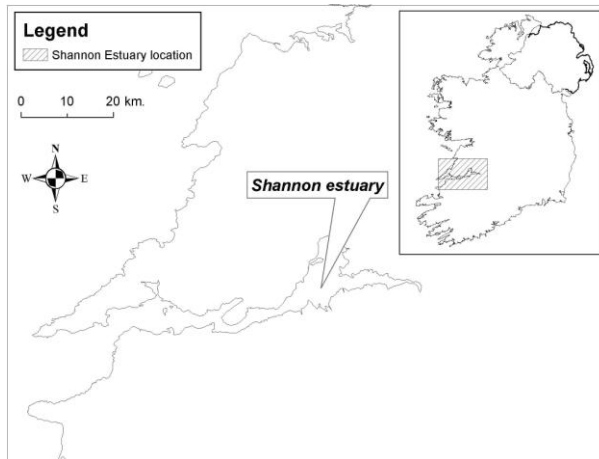

FIG. 1a. Location of the study area (Shannon Estuary in Ireland).

FIG. 1b. Morphology and vegetation makeup in the study area.

GPS surveys

GPS DATA were captured using a Trimble R8 dual-frequency GPS receiver in two separate surveys. Initial surveying was undertaken using FastStatic survey (at a mean sampling resolution of 65 metres) and these data were post-processed using Trimble Geomatics Office (v1·63) software against RINEX correction data on an 18km baseline from the closest geodetic correction station. A second set of GPS points were acquired (after the official launch of the national RTK correction system) using two minute residence-time static RTK survey at a mean horizontal sampling resolution of 18 metres. GPS surveys were conducted on a semi regular grid, capturing at least one point per grid square, each survey being planned in advance and referred to in the field (using a Trimble GeoXT GPS receiver) to guide the dual-frequency survey. Wherever practicable (the soil surface was unsafe in some cases) GPS points were captured at the centre of each grid square. Additional GPS measurements were taken in cases where the slope varied within individual grid squares. GPS error for the RTK points was quantified by reference to the Trimble RTK correction output statistics logged during RTK correction. The combined set of 268 GPS points was used to validate TLS point-cloud error, and a separate set of 20 GPS static RTK points was acquired for the positions of the High Definition Scanning (HDS) laser targets used for TLS point-cloud georeferencing.

TLS survey design and execution

THE TLS DATA were captured using a Leica ScanStation-1 laser scanner in combination with Leica Cyclone 5·7 survey software. The data were captured in 11 separate 360º x 270º scans (scan A1 was repeated to form a back-sight link to the previous 10 scans) and these scans were subsequently co-registered using the centres of the 20 HDS laser targets that were shared between overlapping scans (figure 2). Twelve of the 20 targets were used in clusters of three to co-register the eleven TLS scans into four scan groups. TLS scans were acquired in sets of three

4

because of the range limit for acquiring targets using the Leica ScanStation (tested successfully by authors to ranges of 85m). The remaining eight targets were used to link the four (A,B,C,D) scan groups into a single overall TLS point-cloud mosaic. The range-dependent sampling resolution of the scanner was set in all cases to ensure a minimum of one high-intensity return from all targets. High-intensity returns were then used as seed points to orient 1x1 mm resolution scans of every target face. The Leica Cyclone 5.7 survey software used these detailed scans in conjunction with the verticality (the Leica ScanStation was levelled internally and the target pole was levelled on a bubble) to assign an x,y,z vertex to the centre coordinates of each HDS target. Unique ID codes were assigned to each target during the survey to facilitate target matching during scan co-registration of adjacent overlapping scans.
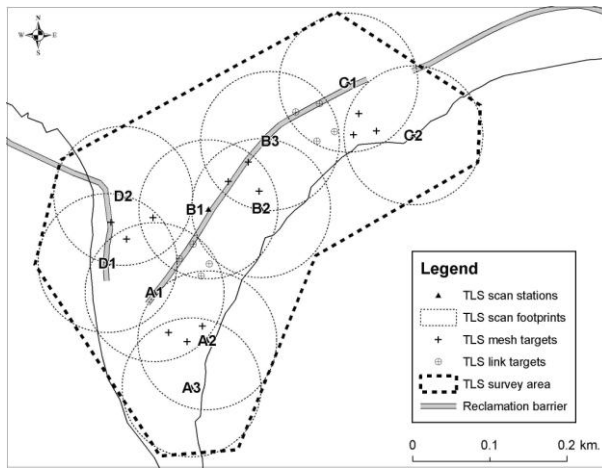

FIG. 2. Minimum footprints of TLS 11 scans (including two location A1).

The overall survey was designed to minimise the number of 360º scans required for full areal coverage, while ensuring that a minimum of three HDS registration targets were detected in every individual scan. A coastal reclamation barrier that flanked the landward limits of the study area provided a 1·5 m tall vantage point for five (including scan A1 twice) of the scans. An additional four scans were taken in the area between the reclamation barrier and the coastline, and a further 2 scans were taken in a flat control area (a newly mown football field) behind the reclamation barrier (figure 2).

Co-registration was done in three stages. The first two stages involved several sub-registrations, and the errors resulting from HDS control point mismatches were quantified for each co-registration. The full TLS point-cloud mosaic was then georeferenced to the GPS positions of the HDS targets; the positions of target centres being measured as vertical offsets from GPS survey pole-point at ground level marked by plum-weight. The positions of the target positions were defined at ground level using two minute static RTK GPS.

5

Elevation errors introduced during georeferencing included inaccuracies in the GPS measurements themselves and errors resulting from the (Affine) geometric transformation applied to georeference the data. The final georeferenced TLS point-cloud mosaic covered 11 hectares of densely-grassed (see tables 4 & 5 for quantification of errors attributable to grass depth) coastal saltmarsh (figure 3) and comprised 27 million x,y,z data points at a mean horizontal sampling resolution of 0·06 m.
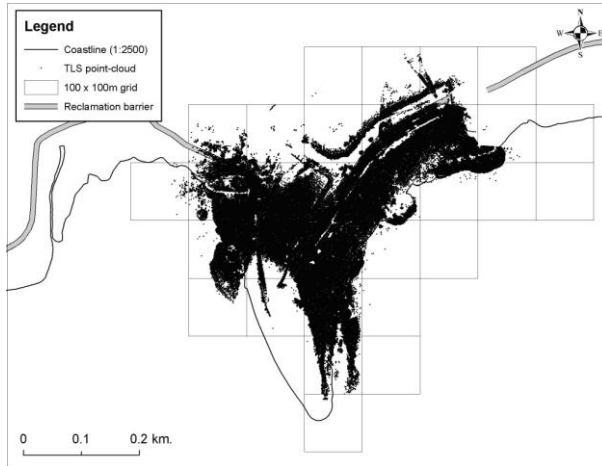

FIG. 3. TLS point-cloud mosaic.

TLS point-cloud error quantification

A NUMBER OF SOURCES contributed to the overall error observed in the TLS point-cloud data. These included GPS measurement error, scan co-registration error, point-cloud georeferencing error, laser target position-definition error, and elevation error caused by the combination of vegetation occlusion and vegetation depth in the TLS data. Errors deriving from these sources were evaluated separately. The methods applied in each case are outlined in the following sub-sections.

GPS MEASUREMENT ERRORS for the overall set of 268 GPS validation points were assessed after combining the post-processing and RTK correction statistics in order to confirm their suitability for the validation of TLS error. Individual scans were co-registered in three stages using a minimum of three shared HDS targets for each sub-registration within each registration stage. Horizontal and vertical registration errors for every sub-registration step in the generation of the full eleven-scan point-cloud mosaic were quantified in the Leica Cyclone 5.7 data processing module using its internal Least Squares fit algorithm.

GEOREFERENCING ERRORS were quantified in the Leica Cyclone 5.7 data processing software module for a range of possible registration point combinations. Georeferencing was applied using the set of points resulting in the lowest horizontal and vertical errors. The accuracy of the Leica ScanStation TLS

6

scanner is quoted by the manufacturers as ±0·006 m (x, y & z) at a range of 100 m (Leica Geosystems, 2007). All scans were taken within this range, so large errors were not expected to derive from this source. A detailed assessment of target position-definition was beyond the scope of this paper, but it was possible to estimate it by comparing the sum of errors from other sources.

Vegetation-derived error

THE SINGLE LARGEST SOURCE of error derived from the sum of vegetation occlusion and vegetation depth in the TLS data. However, it was possible to filter out 99.7% of the erroneous data points from the georeferenced point-cloud before measuring the residual error attributable to these sources. This reduced the resolution of the point-cloud (from 0·06 m to 1 m) while removing all but the lowest elevation point occurring in each metre square of the TLS point-cloud mosaic.

TLS point-cloud filtering

A POLYGON MASK was applied to the georeferenced point-cloud to limit the TLS data to the open, uniformly-vegetated, flood-prone saltmarsh area and its adjacent control area. This reduced the point-cloud area from 11 hectares to 8·5 hectares and the number of TLS data points from 29 million to 22·5 million. Data filtering was then applied to remove local high-points (coinciding with taller vegetation) from the data.

As is the case with all tripod-mounted scanners (Petrie & Toth 2009) the Leica ScanStation operates at a low incidence angle when acquiring topographic data. Therefore, the potential for dense and deep vegetation cover to occlude laser pulse illumination of the bare-ground surface was greater than would normally be expected in nadir-view ALS data. This is because the low incidence angle TLS oblique view resulted in a much longer potential optical path through the vegetation canopy than would have been expected from a vertical view angle.

A Grid Based Elevation Filter (GBEF) was devised to select the lowest local TLS elevation points (one per metre square was chosen in this case) and to filter out all other locally-higher points from the point-cloud mosaic. The GBEF was run in a MySQL database (which handled the 22·5 million-point data-set easily) after assigning a unique 1x1 m grid cell ID to all TLS points. The filter (coded in PERL) ran an SQL query to sequentially select and sort the elevation values in each 1x1 m grid cell, writing the x,y,z record for the lowest elevation value in each 1 m2 cell group (c.250 points in each cell group) to a new MySQL table. The GBEF reduced the point-cloud from 22·5 million points at a mean ground-sampling resolution of 0·06 m to 86,000 points at a mean sampling resolution of 1 m. The choice of 1 m resolution was selected empirically in order to preserve systematic elevation error associated with vegetation prior to measuring it, and in order to preserve topographical details that may have been reflected in the vegetation canopy surface.

Post-GBEF vegetation error

GROUND VEGETATION ERRORS REMAINING in the post-GBEF point-cloud data were quantified using 268 GPS validation points (acquired at a mean ground

7

sampling resolution of 18 metres). Validation was carried out by fitting a universal kriging surface to the TLS point-cloud (in ArcGIS 9.3 Geostatistical Analyst) and validating the surface with the GPS elevation values. Interpolation parameters were optimised in conjunction with cross-validation to minimise the introduction of interpolation error. The maximum error detected in the post-GBEF data was 16 times larger than the single largest non-vegetation error source. This suggested that a very significant error contribution originated from the combined affect of vegetation occlusion and vegetation depth.

Vegetation error adjustment

THE 268 ELEVATION ERROR values highlighted (at mean intervals of 18 m) in the kriged TLS surface model were used to derive a vegetation error model describing the magnitude of vegetation-derived elevation error across the entire TLS coverage. This provided a mechanism for the quantification (and experimental adjustment) of vegetation-derived elevation error at all 86,000 TLS points. The Vegetation Error Model (VEM) was generated by universal kriging using cross-validation to minimise the introduction of interpolation error.

The GPS-derived adjustment of vegetation error was achieved by subtracting the vegetation error values in the VEM model from the TLS point-cloud elevation values. Quantification of residual TLS point-cloud error could not be determined by external validation after adjustment because all available GPS points were used to generate the VEM model. However, the total residual elevation error remaining after VEM adjustment could be estimated by summing the contributions of VEM cross-validation error and GPS measurement error at each of the 18 m resolution external validation points.

<center>RESULTS</center>

GPS measurement error

ELEVATION ERROR STATISTICS were generated for the GPS points during post-processing and RTK correction (FastStatic survey was used for components of GPS survey conducted prior to the formal launch of the Irish RTK correction service). Post-processing errors were quantified in Trimble Geomatics Office software using RINEX (Receiver Independent Exchange format) GPS correction data from the national geodetic correction service. Post-processing and RTK correction was conducted on a short (18km) baseline to the nearest GPS correction station. RTK error statistics were logged to the Trimble survey logger during realtime correction. Ninety-five percent of the combined post-processed and RTK measurement errors at the 268 sampling points were <0·02 m (table 1) making them suitable for the validation of TLS error.

<center>TABLE 1. Elevation error contributions from all individual sources.</center>

Error contributor	Max error (m)	Mean error (m)
Co-registration stage 1	0·007	0·003
Co-registration stage 2	0·011	0·005

Co-registration stage 3	0·012	0·012
GPS validation data error	0·014	<0.001
GPS georeferencing data error	0.003	0.002
Georeferencing error	0·047	0·045
Target position-definition error	0·009	0·009
Arithmetic sum of errors	0.08	Not Applicable

Quantification of TLS point-cloud error

ELEVEN OVERLAPPING TLS SCANS on ten scan footprints (scan A1 was repeated as linking scan with the 10 previous scans) were captured in the test study area (figure 2). Adjacent scans were combined into a single point-cloud mosaic using GPS-controlled high-reflectivity TLS targets. The co-registered TLS point-cloud mosaic was georeferenced to Irish National Grid projected (metres) coordinates and Irish map datum using the national mapping agency geodetic transformation software (Grid Inquest 6.5.2).

TLS scan co-registration error

CO-REGISTRATION of the scans into a single point-cloud mosaic (figure 3) entailed three steps. The first involved co-registration of scan groups centred on sets of 3 'mesh' HDS targets. Overlapping scan groups were then co-registered using sets three 'link' targets (figure 2). The final step involved co-registration of the outputs issuing from stage two to create a single co-registered TLS point-cloud mosaic. Horizontal and vertical errors (resulting from imperfect target matching) during each co-registration step were quantified in the Leica Cyclone 5·7 data processing software. The largest horizontal target mismatch error occurring during co-registration was 0·04 m, and the largest elevation error introduced was 0·014 m (table 1).

TLS point-cloud georeferencing error

THE CO-REGISTERED POINT-CLOUD mosaic (consisting of 27 million points at a mean horizontal sampling resolution of 0·06 m) was georeferenced to the GPS-defined positions of the HDS target centres (measured as offsets from GPS positioning measurements at ground level using a plum-weight) using the Affine transformation georeferencing function in Leica Cyclone 5·7 (which was appropriate since georeferencing involved resizing, rotation and relocation only).

Georeferencing errors came from three sources (namely geometric transformation error, internal GPS measurement errors and HDS target positioning error). A separate (from the GPS validation data) set of 20 static RTK GPS points was used only for georeferencing. These GPS measurements were acquired by means of two minute residence time static RTK survey. The largest internal elevation error that occurred within the georeferencing GPS data was <0·003 m (table 1), and the largest error introduced during georeferencing was <0.05 m (table 2).

TABLE 2. Error margins in the (RTK) GPS used for point-cloud georeferencing.

Georeferencing point ID	Horizontal error (m)	Elevation error (m)
ct_4	±0·038	±0·004
bcl_4	±0·034	±0·018
abl_4	±0·034	±0·033
dt_2	±0·036	±0·047

In terms of georeferencing errors introduced during geometric (Affine) transformation in Leica Cyclone 5.7, the errors deriving from use of 3, 4, 5, 6 & 7 georeferencing points were pre-tested (table 3) prior to georeferencing. A four-point georeferencing based on a wide rectangular ground spread of HDS target georeferencing points produced the lowest maximum and mean georeferencing errors (table 3) so these four-points were used to georeference the point-cloud mosaic. Offsets between the original positions of HDS target centres and their positions after georeferencing were output as combined horizontal / vertical offset vectors for each HDS target position in the Leica Cyclone 5.7 data processing module. The minimum error introduced during geometric transformation was 0·4cm, the maximum error was 4·7cm, and the mean error was 4·5cm.

TABLE 3. ACCURACY STATISTICS FOR TESTED GEOMETRIC TRANSFORMATIONS.

Georeferencing points	Minimum error (m)	Maximum error (m)	Mean error (m)
3	0·003	0·052	0·047
4	0·004	0·047	0·045
5	0·009	0·052	0·048
6	0·003	0·058	0·051
7	0	0·057	0·057

Some additional errors were expected to derive from HDS scan positioning error because the absolute positions of the HDS target centres (mounted on levelled tripods) were defined as measured vertical displacements (by plum-weight and measuring tape) from the marked positions of the GPS measurements at ground-level. However, it was not possible to validate these errors directly and measuring the difference between the pre and post georeferencing positions of the remaining 16 target positions would have reflected the dominant influence of geometric transformation error. Therefore, particular care was taken when physically measuring the vertical displacements of the HDS targets from ground level to ensure these errors were kept to <1cm.

TLS point-cloud filtering

THE DEPTH OF THE GROUND VEGETATION in the study area indicated that this was likely to be a large source of error in the TLS point-cloud mosaic. The TLS data were filtered before error testing was carried out. Since the geo-registered

point-cloud mosaic contained extraneous laser returns from outside the limits of the open uniformly-vegetated survey area (from trees and high ground) extraneous areas were removed from the georeferenced point-cloud mosaic by simply masking off unwanted areas. This reduced the size of the point-cloud mosaic to approximately 8·5 hectares and 22·5 million points and confined its extent to the open uniformly-vegetated saltmarsh and its adjacent control area (figure 4).

As noted previously, the ScanStation TLS scanner was not capable of segregating first and last laser returns, so the georeferenced point-cloud contained many returns from tall vegetation. However, it was possible to remove some of the TLS returns that coincided with taller vegetation stems. A Grid-Based Elevation Filter (GBEF) was devised to select out the single local lowest TLS point (per square metre) and to remove the remaining 99·6% of the points from the point-cloud mosaic. This reduced the mean resolution of the point-cloud mosaic 250/m2 to 1 m2, and reduced the number of TLS points from 22·5 million to 86,000 points (figure 4).

Generally-speaking the GBEF worked very well. However, a small number of 'negative-sign' errors (i.e. where the local lowest point was at a lower elevation than its closest GPS validation point) occurred in 33 locations coinciding with the sloping flanks of a reclamation barrier that delineated the northern edge of the main survey area (figure 2). These occurred where the GBEF filter selected points on the lower edge of sloped 1 m GBEF grid cells on the flanks of the reclamation barrier. These 33 errors were a simply a function of the operation of the GBEF filter and did not represent actual TLS data errors, so they were removed from all subsequent error assessments. All other errors highlighted by external validation were 'positive sign' errors, reflecting the influence of laser returns from vegetation.
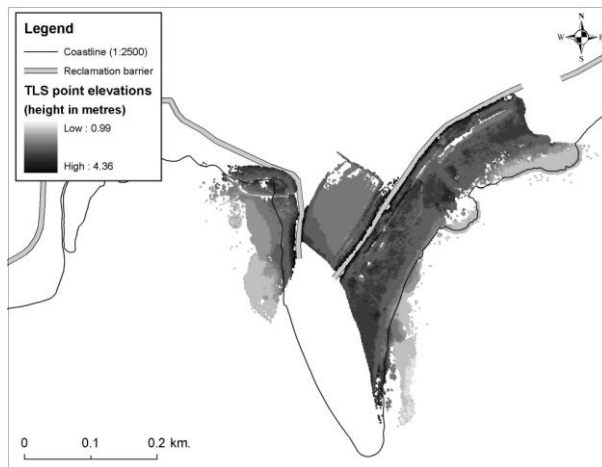

FIG. 4. Post-GBEF filtered TLS point-cloud.

Post-GBEF vegetation error

THE REMAINING 235 VALIDATION DATA values (after removal of the 33 reclamation barrier points) provided a set of vegetation error values at a mean ground sampling resolution of 19 metres across the rest of the post-GBEF point-cloud. The Standard Deviation of the post-GBEF elevation errors highlighted by GPS validation was 0·39 m, but the maximum elevation error of 1·31 m noted in the data indicated that substantial vegetation-derived elevation errors remained in the data (table 4).

TABLE 4. Elevation errors in the main survey and control areas after removal of post-GBEF elevation anomalies.

Measures	Entire TLS area	Control area
Validation points	235	114
Negative outlier	None	None
Positive outlier	1·31 m	0·38 m
Mean elevation error	0·33 m	0·09 m
95% elevation error	0·98 m	0·15 m

The mean sampling resolution (19 m) and spacing of the remaining 235 error measurements provided a representation of the spatial distribution of vegetation error across the substantially flat survey area (figure 5). However, it also made it possible to generate a 2·5D Vegetation-Error Model (VEM) by kriging the error values for the entire study area (figure 6). This VEM could then be used to experimentally adjust TLS vegetation error in order to provide an estimate of vegetation-derived error at every TLS data point and to highlight the magnitude of vegetation error in comparison to the other error sources examined.
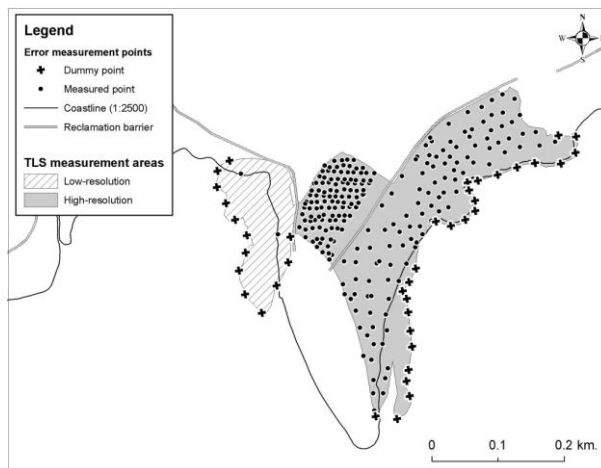
Vegetation error adjustment

THE 235 GPS-DERIVED TLS ERROR measurements were well spread across the study area but were relatively thinly distributed around the perimeter of the study area, so a set of dummy values were added to smooth the interpolation of the vegetation-error point values out to the edge of the study area (figure 6). Elevation point values for the dummy points were estimated by assigning them the height value of their nearest measured neighbour. The use of these dummy values was a relatively crude mechanism but it did help to offset the tendency for substantial edge errors (Lindsay & Creed, 2005) to be introduced during interpolation of the VEM point error values. The 235 error measurements were combined with 40 dummy vegetation-error values and were interpolated using universal kriging (using the same approach as in previous cases) to generate the VEM (figure 6).

The adjustment of vegetation error simply involved subtraction of the VEM values from the TLS point-cloud elevation measurements (in ArcGIS 9.3 Geostatistical Analyst). Subtraction was carried out by externally validating the continuous VEM 2·5D surface with the post-GBEF TLS point-cloud elevation values. The residuals from this corresponded with the estimated ground elevations at every TLS point in the theoretical absence of ground vegetation cover.
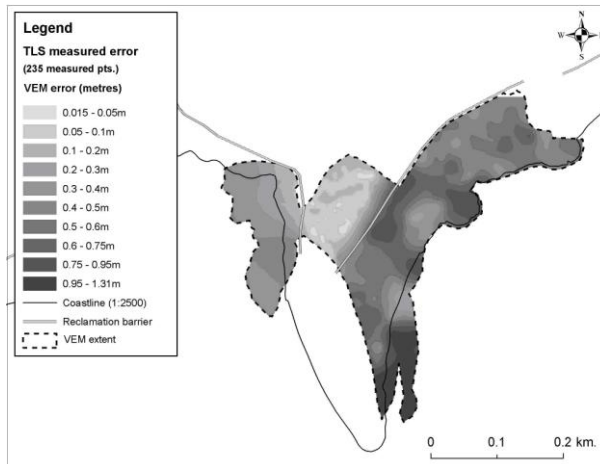

Fig. 6. VEM model.

Quantifying residual vegetation derived error

NO GPS DATA were available for external validation of the error-adjusted TLS point data so residual errors after application of the VEM adjustment had to be inferred by other means. Total residual error was estimated by summing the accuracy errors in the GPS point measurements and errors highlighted during Leave-One-Out-Cross-Validation (LOOCV) of the interpolation of the 235 VEM

point error values. Using LOOCV values as an estimate for VEM model error probably overstated (rather than underestimated) actual error due to the local reduction of sampling resolution that occurs during LOOCV cross-validation.

Defining the cumulative error from these sources was a straightforward matter. Errors deriving from each source were simply added at each of the 235 sample points to generate a new set of 235 error quantities (table 5). Because some of the errors from these error sources offset one another, the cumulative error from both sources turned out to be no larger than the errors from the largest error contributor (i.e. the VEM interpolation cross-validation errors). Ninety percent of the elevation errors highlighted by LOOCV were in the range of ±0·2 m (95% of errors were within the ±0·275 m range). The standard deviation of all the errors was 0·12 m (table 5).

TABLE 5. Cumulative error from GPS measurements and VEM cross-validation.

Point count	235
Maximum negative-sign error	-0·46 m
Maximum positive-sign error	0·57 m
Standard deviation	0·12 m
90% elevation error	±0·2 m
95% elevation error	±0·275 m

Target position-definition error

SCANNER RANGING ERROR was not assessed in a laboratory context, but it was possible to attempt an estimate of target position-definition error by comparing validated elevation in the control area (a newly-mown and football field) with measured vegetation error in this area. A subset of 114 GPS points (from the total set of 235) located within the control area (figure 5) were used to measure elevation error, highlighting 95th percentile error of 0·15 m (no negative sign errors were evident in this case) and a mean error of 0·09 m (table 4). Vegetation height was not measured at every fifth GPS point (yielding a total of 25 measurements) indicating vegetation heights of 0·04 - 0·14 m, and a vegetation height of 0.08 m.

The similarity of the externally validated error and the vegetation depth measurements indicated that the primary source of elevation error in the control area was occlusion of the ground surface by vegetation. As was the case elsewhere in the study area, the measured error values included errors deriving from vegetation occlusion, GPS positioning, target mismatching (co-registration), georegistration (Affine transformation) and laser ranging error. However, since the sum of all error sources was close to that of the vegetation height values, it was not possible to isolate the component contribution of target position-definition error, or ranging accuracy.

THIS PAPER has attempted to quantify the potential contribution to TLS elevation error deriving from the presence of deep and dense ground vegetation cover in natural areas, and to compare the magnitude of these errors with inaccuracies resulting from TLS surveying and data processing. The intention was to highlight the extent to which ground vegetation error can affect TLS accuracy, even in situations where TLS data are acquired and processed with a high degree of accuracy control. The study was applied to TLS data acquired in a flat, open, densely-vegetated coastal saltmarsh grassland area, which provided an opportunity to assess the degree to which vegetation affects elevation error in a situation where other sources of error (namely: topographic variability, trees or shrubs) were minimised.

The contributions to TLS error deriving from GPS measurement, scan co-registration, georeferencing, laser target position-definition error and the affect of TLS occlusion by ground vegetation cover were quantified separately. The maximum errors attributable to internal GPS measurement error (0·014 m), scan co-registration error (0·04 m) and georeferencing error (0.047 m) were all very small compared to TLS point-cloud error. The maximum elevation error of 0.38 m in the post-GBEF TLS data (table 4) was 8 times larger than the largest single survey-derived error input, and almost 5 times the arithmetic sum (assuming none of these offset one another to any degree) of all these separate error sources. The magnitude of this differential demonstrated the potential for vegetation-derived error to significantly affect ground representation accuracy even in situations where flat open terrain prevails, and in the absence of large occluding vegetation features such as trees and shrubs.

The availability of GPS data at a relatively high horizontal sampling resolution made it possible to validate elevation error at a relatively large number of individual locations (235 in total). However, it also enabled the magnitude of the elevation error at all 86,000 TLS points to be inferred, as well as facilitating the experimental adjustment of vegetation-derived TLS error. The VEM error adjustment applied to the post-GBEF point-cloud data reduced elevation error overall by about 40%. However, while the Geostatistics-based data fusion of TLS and GPS worked satisfactorily in the context of highlighting the potential magnitude of elevation error attributable to the presence of ground vegetation cover, it is not advanced as a solution to the problem of vegetation error in TLS data (due to the amount of work required to achieve this). Rather, it demonstrates the limitations of TLS in open areas where dense ground vegetation predominates.

One issue that was not examined was the degree to which the problem would manifest itself if waveform TLS had been used. It is likely that the problem of significant lateral canopy depth resulting from the generally low incidence angle (at all but very near ranges) afforded by tripod-mounted TLS would have been a problem regardless of the TLS instrument used. However, this appears to remain an open question.

CONCLUDING REMARKS

ELEVATION ERROR ASSOCIATED WITH GROUND VEGETATION in the single-returns TLS data (after the application of local elevation filtering) was 16 times larger than elevation errors deriving from the single largest survey or data processing error source. The vegetation-derived error was also approximately 5 times the magnitude of the arithmetic sum of all survey-derived errors (assuming none of these offset one another) combined. Error deriving from GPS error (<3cm), scan co-registration error (<4cm), geo-registration error (<5cm) and laser target position-definition error (~5cm) confirmed that the total elevation observed was substantially derived from the presence of ground vegetation.

The GBEF filter proved to be a simple and effective mechanism for the removal of local elevation error in the single-returns TLS data. Given the manner in which the GBEF filter operates (i.e. selection of the local lowest elevation point in a user-defined x, y cell dimension) it is possible that further reductions in elevation error could have been achieved if the filter was applied at a lower spatial resolution. However, in this case, the 1 m resolution preserved topographic model detail that would have been lost at lower resolutions.

Further reductions in TLS elevation error were achieved with the application of the VEM adjustment. The geostatistics-based data fusion of TLS and GPS data fusion that was used to generate the 2·5D VEM correction provided an additional mechanism to highlight the contribution of vegetation error (based on its successful removal). However, given the relatively large number of GPS points that were required for the VEM-based adjustment of TLS elevation error, this is not being advanced here as a solution to the problem of vegetation error in TLS data. The use of these GPS data for DEM generation has been demonstrated in a parallel study (Coveney, *In Press*), suggesting that GPS may offer a workable alternative to TLS in situations where large scale bare-earth DEMs are required in the absence of ALS data.

REFERENCES

BALDI, P., BONVALOT, S., BRIOLE, P., COLTELLI, M., GWINNER, K., MARSELLA, M., PUGLISI, G. AND RÉMY, D., 2002. Validation and comparison of different techniques for the derivation of digital elevation models and volcanic monitoring, Vulcano Island, Italy. *International Journal of Remote Sensing,* 23(22): 4783-4800.

BUCKLEY, S. J., HOWELL, J. A., ENGE, H. D. AND KURZ, T.H., 2008. Terrestrial laser scanning in geology: data acquisition, processing and accuracy considerations. *Journal of the Geological Society,* London, 165: 625–638.

COVENEY, S., FOTHERINGHAM, S, CHARLTON, M. AND MCCARTHY, T., 2010. Dual-scale validation of a medium-resolution coastal DEM with Terrestrial LiDAR DSM and GPS. *Computers and Geosciences,* 36: 489–499.

DANSON, F. M., HETHERINGTON, D., MORSDORF, F., KOETZ, B. AND ALLGÖWER, B., 2007. Forest Canopy Gap Fraction from Terrestrial Laser Scanning. *IEEE Geoscience and Remote Sensing Letters,* 4(1): 157-160.

FLOOD, M., 2004. ASPRS Guidelines - Vertical Accuracy Reporting for LiDAR Data, version 1·0. *American Society of Photogrammetry and Remote Sensing LiDAR Committee (PAD).* 20 pages (http://www.asprs.org/society/committees/lidar/downloads/vertical_accuracy_reporting_for_lidar_data.pdf on 20th April, 2011).

FULLER-ROWELL, T., 2005. USTEC: A new product from the Space Environment Centre characterizing the ionospheric total electron content. *GPS Solutions,* 9: 236-239.

GAO, Y. AND CHEN K., 2004. Performance Analysis of Precise Point Positioning Using Real-Time Orbit and Clock Products. *Journal of Global Positioning Systems,* 3(1-2): 95-100.

GORTE, B., PFEIFER, N. AND OUDE ELBERINK, S., 2005. Height Texture of Low Vegetation in Airborne Laser Scanner Data and its Potential for DTM Correction. *The International archives of Photogrammetry, Remote Sensing and Spatial Information Sciences,* XXXVI, (3/W19), 150-155.

GUARNIERI, A., VETTORE, A., PIROTTI, F., MENENTI, M. AND MARANI, M., 2009. Retrieval of small-relief marsh morphology from Terrestrial Laser Scanner, optimal spatial filtering, and laser return intensity. *Geomorphology,* 113: 12–20.

HALL, S. A., BURKE, I. C., BOX, D. O., KAUFMANN, M. R. AND STOKER, J. M., 2005. Estimating stand structure using discrete-return LiDAR: An example from low density, fire prone ponderosa pine forests. *Forest Ecology and Management,* 208: 189-209.

HENNING, J.G. AND RADTKE, P.J., 2006. Ground-based Laser Imaging for Assessing Three-dimensional Forest Canopy Structure. *Photogrammetric Engineering & Remote Sensing,* 72(12): 1349–1358.

HERITAGE, G. AND HETHERINGTON, D., 2007. Towards a protocol for laser scanning in fluvial Geomorphology. *Earth Surface Processes and Landforms,* 32: 66–74.

HÖHLE, J. AND POTUCKOVA, M., 2006. The EuroSDR Test: Checking and Improving of Digital Terrain Models. *(In) EuroSDR European Spatial Data Research, Official Publication No. 51*, EuroSDR Publications, Frankfurt, Germany. 188 pages: 9-141. (http://www.eurosdr.net/publications/51.pdf on 20th April 2011)

LEICA GEOSYSTEMS, 2007. *High Definition Surveying: Training Manual, Leica Geosystems*, Munich, Germany. 2 pages (http://hds.leica-geosystems.com/downloads123/hds/hds/ScanStation/brochures-datasheet/Leica_ScanStation%202_datasheet_us.pdf on 20th April, 2011).

LIM, K., TREITZ, P., WULDER, M., ST-ONGE, B. AND FLOOD, M., 2003. LiDAR remote sensing of forest structure. *Progress in Physical Geography,* 27(1): 88-106.

LINDSAY, J. B. AND CREED, I. F., 2005. Removal of artifact depressions from digital elevation models: towards a minimum impact approach. *Hydrological Processes,* 19: 3113-3126.

NAYEGANDHI, A., BROCK, J. C., WRIGHT, C. W. AND O'CONNELL, M. J., 2006. Evaluating a small footprint, waveform-resolving LiDAR over coastal vegetation communities. *Photogrammetric Engineering and Remote Sensing,* 72: 1407–1417.

OKSANEN, J. & SARJAKOSKI, T., 2005. Error propagation analysis of DEM-based drainage basin delineation. *International Journal of Remote Sensing,* 26(14): 3085-3102.

PETRIE, G. AND TOTH, C.K., 2009. Terrestrial Laser Scanners. In: *Topographic Laser Ranging and Scanning: Principles and Processing,* (Eds. J. Shan and C. K. Toth) CRC Press, Taylor and Francis Group, Florida, USA. 590 pages: 87-128.

PFEIFER, N. AND BRIESE, C., 2007. Geometrical Aspects of Airborne Laser Scanning and Terrestrial Laser Scanning. *International Archives of Photogrammetry and Remote Sensing,* XXXVI (3/W52), 311–319.

PFEIFER, N., GORTE, B., AND OUDE ELBERINK, S., 2004. Influences of Vegetation on Laser Altimetry - Analysis and Correction Approaches. In: M. Thies, B. Koch, H. Spiecker and H. Weinacker (Editors), *Proceedings of Natscan, Laser-Scanners for Forest and Landscape Assessment - Instruments, Processing Methods and Applications. International Archives of Photogrammetry and Remote Sensing,* XXXVI, (8/W2): 283-28.

PU, S. AND VOSSELMAN, G., 2009. Knowledge based reconstruction of building models from terrestrial laser scanning data. *ISPRS Journal of Photogrammetry and Remote Sensing,* 64: 575-584.

ROSSER, N. J., PETLEY, D. N., LIM, M., DUNNING, S. A. AND ALLISON, R. J., 2005. Terrestrial Laser Scanning for monitoring the process of hard rock coastal cliff erosion. *Quarterly Journal of Engineering Geology and Hydrogeology,* 38: 363–375.

SCHARDT, M., ZIEGLER, M., WIMMER, A., WACK, R., & HYYPPA, J., 2002. Assessment of forest parameters by means of laser scanning. *The International Archives of the Photogrammetry, Remote Sensing and Spatial Information Sciences,* XXXIV, (3A): 302-309.

STRAATSMA, M. W., WARMINK, J. AND MIDDELKOOP, H., 2008. Two novel methods for field measurements of hydrodynamic density of floodplain vegetation using terrestrial laser scanning and digital parallel photography. *International Journal of Remote Sensing,* 29(5): 1595-1617.

THIES, M. AND SPIECKER, H., 2005. Evaluation and Future Prospects of Terrestrial Laser Scanning for Standardized Forest Inventories. *International Archives of Photogrammetry, Remote Sensing and Spatial Information Sciences,* XXXVI(8/W2): 192-197.

VOSSELMAN, G., GORTE, B., SITHOLE, G., RABBANI, T., 2004. Recognizing structure in laser scanner point clouds. *International Archives of Photogrammetry, Remote Sensing and Spatial Information Sciences,* 46 (8/W2): 33-38.

WAGNER, W., HOLLAUS, M., BRIESE, C. & DUCIC, V., 2008. 3D vegetation mapping using small-footprint full-waveform airborne laser scanners. *International Journal of Remote Sensing,* 29, 5, 1433–1452.

WEBSTER, T. L., 2005. LiDAR Validation Using GIS: A Case Study Comparison between town LIDAR Collection Methods. *Geocarto International,* 20(4): 11-19.

WEBSTER, T. L., FORBES, D. L., MACKINNON, E. AND ROBERTS, D., 2006. Flood-risk mapping for storm-surge events and sea-level rise using LiDAR for southeast New Brunswick. *Canadian Journal of Remote Sensing,* 32(2): 194-211.

Résumé

Space for insertion of relevant text later under guidance of editor.

Zusammenfassung

Space for insertion of relevant text later under guidance of editor.